A fresh look at dense hydrogen under pressure. III. Two competing effects and the resulting intra-molecular H-H separation in solid hydrogen under pressure

Vanessa Labet, Roald Hoffmann, and N. W. Ashcroft

Citation: J. Chem. Phys. **136**, 074503 (2012); doi: 10.1063/1.3679749
View online: http://dx.doi.org/10.1063/1.3679749
View Table of Contents: http://jcp.aip.org/resource/1/JCPSA6/v136/i7
Published by the American Institute of Physics.

A fresh look at dense hydrogen under pressure. III. Two competing effects and the resulting intra-molecular H-H separation in solid hydrogen under pressure

Vanessa Labet,[1,a)] Roald Hoffmann,[1,b)] and N. W. Ashcroft[2]
[1]*Department of Chemistry and Chemical Biology, Cornell University, Baker Laboratory, Ithaca, New York 14853, USA*
[2]*Laboratory of Atomic and Solid State Physics and Cornell Center for Materials Research, Cornell University, Clark Hall, Ithaca, New York 14853, USA*

(Received 19 September 2011; accepted 6 January 2012; published online 15 February 2012)

A preliminary discussion of the general problem of localization of wave functions, and the way it is approached in theoretical condensed matter physics (Wannier functions) and theoretical chemistry (localized or fragment orbitals) is followed by an application of the ideas of Paper II in this series to the structures of hydrogen as they evolve under increasing pressure. The idea that emerges is that of simultaneously operative physical (reduction of available space by an increasingly stiff wall of neighboring molecules) and chemical (depopulation of the σ_g bonding molecular orbital of H_2, and population of the antibonding σ_u* MO) factors. The two effects work in the same direction of reducing the intermolecular separation as the pressure increases, but compete, working in opposite directions, in their effect on the intramolecular (nearest neighbor, intra-pair) distance. We examine the population of σ_g and σ_u* MOs in our numerical laboratory, as well as the total electron transfer (small), and polarization (moderate, where allowed by symmetry) of the component H_2 molecules. From a molecular model of two interacting H_2 molecules we find a linear relationship between the electron transfer from σ_g to σ_u* of a hydrogen molecular fragment and the intramolecular H-H separation, and that, in turn, allows us to estimate the expected bond lengths in H_2 under pressure if the first effect (that of simple confinement) was absent. In essence, the intramolecular H-H separations under pressure are much shorter than they would be, were there no physical/confinement effect. We then use this knowledge to understand how the separate *E* and *PV* terms contribute to hydrogen phase changes with increasing pressure. © *2012 American Institute of Physics*. [http://dx.doi.org/10.1063/1.3679749]

I. INTRODUCTION

The "simplest things" often turn out to be far from simple. One might think we would know experimentally (and be able to calculate theoretically) just about everything one would want to discover about the behavior of elemental hydrogen under atmospheric conditions and also under pressure. The quest for metallic hydrogen[1] has led physicists and chemists to a large body of excellent experimental research on hydrogen under pressure, some of it summarized in earlier papers in this series.[2] What we have so far, however, is hard-won but piecewise knowledge and understanding.

The demonstrable presence in compressed crystalline hydrogen, of rotons and vibrons to at least 250 GPa itself testifies to the persistence of molecular units, paired protons, and associated electrons, with their characteristic quantized rotations and vibrations. From the analyses of these rotons[3–5] and vibrons[6,7] it has been deduced that the intramolecular H-H bonds shorten and also stiffen from 1 atm to ∼30 GPa, but then both lengthen and weaken from 30 GPa to at least 316 GPa, with a significant discontinuity at 150 GPa (at low temperature), this pressure corresponding to the transition between the broken symmetry phase and the H-*A* phase, also known as Phases II and III, respectively.[8] The overall magnitude of the effect is not large, just on the order of several hundredths of an angström in terms of average separation. But it is quite reproducible.

In the first paper of this series,[2] we analyzed the evolution of the shortest and second shortest proton-proton separations in those structures recently proposed by Pickard and Needs[9] to be the most stable in their comprehensive theoretical study of the phase diagram for crystalline hydrogen below P = 500 GPa (in its ground state and for static arrangements). The structures, labeled by their space groups, are illustrated in Figures 1 and 2; in Table I is indicated the associated pressure range of stability.

In the $P6_3/m$, $C2/c$, *Cmca*-12, and *Cmca* structures, shown in Figure 1, each proton has just one closest neighbor. As discussed in Paper I,[2] even at the highest pressures studied theoretically (490 GPa), the ratio of the next nearest neighbor distance to the closest neighbor is still ∼1.33. Thus, these four structures can be thought of as being molecular or paired (even if the electrons in these dense structures are far from localized; and more of this anon). We will refer to the shortest and second shortest proton-proton separations in these as the intramolecular and shortest intermolecular H-H distances, respectively. In contrast to this, in the high-pressure $I4_1/amd$ structure, shown in Figure 2, each proton actually has four

a)Present address: LADIR (UMR 7075 CNRS/UPMC), Université Pierre et Marie Curie, 4 Place Jussieu, 75252 Paris Cedex 05, France.
b)Author to whom correspondence should be addressed. Electronic mail: rh34@cornell.edu.

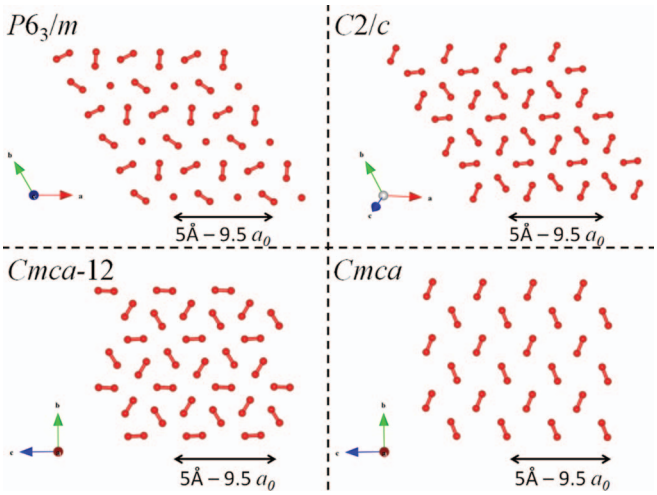

FIG. 1. A layer of the static $P6_3/m$, $C2/c$, *Cmca*-12, and *Cmca* structures at $P = 300$ GPa ($r_s \sim 1.33$). In the $P6_3/m$, *Cmca*-12, and *Cmca* structures the layers are arranged in an ABA fashion; in the $C2/c$ structure they are arranged in an ABCDA fashion.

closest neighbors. Thus the $I4_1/amd$ structure corresponds to a monatomic phase.

By following the most stable structure as pressure increases, we observed that the shortest intermolecular H-H separation decreases uniformly with pressure. The intramolecular H-H separation also starts decreasing, but then increases (in agreement with the experimental evidence), and at very high pressure it then decreases again. The overall variation in intramolecular separation is small over a large pressure range. An index $\xi(P)$ was proposed in the first paper of this series to gauge the equalization of the two distinct kinds of H-H separations with pressure.[2]

In the second paper of this series,[10] we also presented two model structures for the evolution of the intramolecular H-H separation with pressure. Simple confinement of H_2 molecules results only in a diminution of the intramolecular H-H separation and an associated increase in force constant for eventual vibrational motion. Set against this are orbital effects – population upon compression of the σ_u* MOs of the starting H_2 units by electrons and concomitant depopulation of the σ_g orbitals together act to elongate the intramolecular

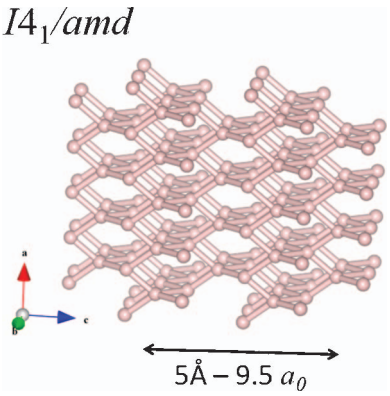

FIG. 2. View of the $I4_1/amd$ structure at $P = 500$ GPa ($r_s \sim 1.23$). Note that each proton is 4-coordinated.

TABLE I. Structures found to be the most stable by Pickard and Needs[9] for dense solid hydrogen up to 500 GPa, in the static lattice-approximation.

Pressure range (GPa)	Symmetry of the most stable structure
<105	$P6_3/m$
105–270	$C2/c$[a]
270–385	*Cmca*-12
385 – 490	*Cmca*
>490	$I4_1/amd$

[a]When the zero-point motion is taken into account, the $C2/c$ structure stability region is shifted from <75 GPa to ~240 GPa.

H-H bond. The objective of the present paper is to further examine how these two effects compete. Once again, we choose the structures proposed by Pickard and Needs[9] as a numerical laboratory in our approach to determine the essence of the underlying physics and chemistry.

II. COMPUTATIONAL DETAILS

The structures proposed by Pickard and Needs to be the most stable for solid hydrogen in its ground state and up to P = 500 GPa, were optimized in the static lattice approximation, as reported in the first paper of this series.[2] We used the Vienna *ab-initio* simulation package (VASP) plane wave code,[11–13] the Perdew-Burke-Ernzerhof (PBE) generalized gradient approximation density functional,[14,15] and the projector augmented-wave method[16,17] with a pseudopotential characterized by a cut-off radius of 0.8 a_0 (a_0 being the Bohr radius), and a cut-off of 2000 eV for the kinetic energy of the plane waves.

As already mentioned in the first paper of this series,[2] with this methodology, the cusp theorem cannot be satisfied. Nonetheless, McMahon and Ceperley[18] have recently shown in their theoretical study of atomic hydrogen between P = 500 GPa and P = 5 TPa, that a cut-off radius of 0.5 a_0 is a reasonable approximation. They came to this conclusion by comparing the energies and electron densities of several structures computed with two choices of pseudopotential radius: 0.5 a_0 and 0.125 a_0. Since we are studying hydrogen at lower pressures than McMahon and Ceperley, we consider that our choice of a pseudopotential cut-off radius of 0.8 a_0 – the smallest available in VASP – is reasonable. In each case, the cell shape and volume were allowed to change and the protons to relax, leading eventually to very small deviation with respect to the group symmetry used to label the structures. The **k**-point sets for the Brillouin-zone sampling were generated via the Monkhorst-Pack scheme.[19] A different set was used for each structure at each pressure, in order to have in each case a grid of spacing of $2\pi \times 0.02$ Å^{-1}. As was the case earlier, we have not included dynamical effects.

A fragment molecular orbital analysis of those optimized structures has been performed using the extended Hückel method,[20] a semi-empirical molecular orbital method whose assumptions are related to the tight-binding model, as implemented in the BIND program distributed in the standard YAeHMOP package.[21]

To establish in the absence of external pressure the correlation between intramolecular H-H separations and the σ_g and σ_u* H_2 fragment MO population, we used a discrete molecular model, which will be presented later. The geometry of this system was also optimized within density functional theory (DFT), using the same PBE density functional used for the optimization of the extended structures, and in association with the triple-zeta 6-311++G(d,p) basis set, as implemented in the GAUSSIAN 03 program.[22]

III. DELOCALIZED AND LOCALIZED VIEWPOINTS IN DENSE HYDROGEN

In the gas phase one has for H_2 (or indeed any molecule) essentially isolated molecular entities, where the scale of the ratio of inter- to intramolecular separations being typically around ∼10 at 1 atm. In the one atmosphere but also low temperature molecular solid, this ratio of separations declines substantially. And under elevated pressure, and as we saw in Paper I,[2] the ratio of next-nearest to nearest H-H separation is already down to ∼1.33 at P = 490 GPa.

Clearly, the average separations in the gas are such that one can talk sensibly of molecules, interacting at long range with other molecules through electrostatic (quadrupole-quadrupole being the leading term for H_2) and London dispersion forces. The band structure of the weakly overlapping P = 1 atm solid (to the extent that this can be defined for a rotational system) is not expected to exhibit any notable features; the important bands formed from σ_g and σ_u* molecular levels have small dispersions. But in the P = 490 GPa solid, now at upwards of 10-fold compression, the orbitals of neighboring H_2 molecules overlap significantly. The width of the bands spreading out from what were at lower pressures discrete σ_g and σ_u* levels is of the order of several eV, and in fact becomes comparable, as metallization approaches, to the separation between the σ_g and σ_u* orbitals in the free molecule (see Fig. 3).

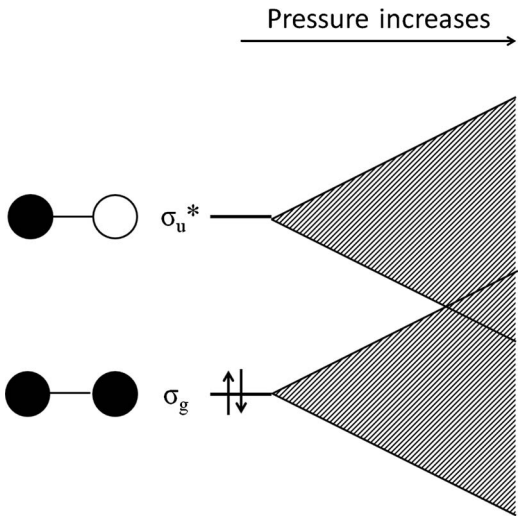

FIG. 3. Schematic view of bands developing from a molecular hydrogen orbital view starting point, as pressure is applied. Dark and light areas denote opposite phases of the wave function.

Accordingly, does it also make sense to talk then of H-H bonds, when the bands are so wide? The answer, we believe, is "yes" but nevertheless with a strong caution.

First, let us point out that there are really two questions here:

(a) Can one describe a delocalized wave function, whether a plane-wave expansion of a crystal wave function, or a crystal molecular orbital (a linear combination of atomic orbitals (LCAO) and also a Bloch function) in terms of wave functions/orbitals of localized units in the crystal? These localized units could be orbitals on an atom, or they could be molecular orbitals, for instance the orbitals σ_g and σ_u*, of a H_2 piece of the crystal.
(b) Do the ensuing localized wave functions have physical meaning?

The answer to the first question is simply "yes." Thinking in a LCAO way, the symmetry adapted (i.e., Bloch function) trial wave function $\psi_{\vec{k}}$ is usually written, un-normalized, in terms of atomic orbitals as

$$\psi_{\vec{k}} = \sum_i e^{i\vec{k}\cdot\vec{R}_i}\phi_i,$$

where overlap is omitted in the normalization. For the simplest (we can do better) such wave function, the AOs ϕ_i are hydrogenic 1*s* functions. If we choose a H_2 unit within the crystal, say from atoms *i* and *i*+1, and form its σ_g and σ_u* MOs, labeled by a molecule index *j*, as follows (again normalized without overlap):

$$\sigma^*_{u,j} = \frac{1}{\sqrt{2}}(\phi_i - \phi_{i+1}),$$

$$\sigma_{g,j} = \frac{1}{\sqrt{2}}(\phi_i + \phi_{i+1}),$$

then it is simply a matter of a rotation, a unitary transformation, to rewrite the wave function for the system in terms of Bloch function expansions of σ_g and σ_u* (and again un-normalized):

$$\psi_{\vec{k}} = \sum_j \sum_{\alpha=g,u} e^{i\vec{k}\cdot\vec{R}_j}\sigma_{\alpha,j}.$$

There is no physics in this transformation; no observable is affected by such a transformation.

The answer to (b) is much more subtle. The question of localization has been faced, albeit in different languages, in both chemistry and physics over the past 70 years. In chemistry, very early on one began to think about localization, driven by a hundred years of experience of atoms in molecules, bonds between atoms, and successful additivity rules by which energies or dipole moments (just to name two observables), could be related to bond energies or bond dipoles. There evolved not just one, but several localization schemes – for instance, one which minimizes the electron repulsion between the localized orbitals.[23–27]

A general consensus that has emerged in chemistry is the following: (1) Calculations which use the localized orbitals as a transferrable (from molecule to molecule) basis for a many electron calculation are not very effective. (2) Observables

which depend on all the electrons in a molecule (e.g., dipole moment, total energy) can be equally well interpreted within a localized orbital scheme as in a delocalized one – the latter are the so-called canonical orbitals. But for properties that depend on one MO, or a subset of MOs (e.g., ionization potentials, spectra, etc.), one has to work in the delocalized or canonical orbital perspective.

In condensed matter physics, the analogous discussion focuses on the Wannier functions,[28–30] going back to 1937 (the birth year of the older author of this paper). These are unitary transformations of the Bloch functions $\psi_{\vec{k}}$, sums over the first Brillouin zone,

$$\phi_i = \sum_{\vec{k}} e^{-i\vec{k}\cdot\vec{R}_i}\psi_{\vec{k}}.$$

In contrast to the tight-binding atomic-like functions, these functions, the Wannier functions, constitute a complete orthogonal set and they provide us with an alternative basis for a description of the independent electron levels of dense crystalline hydrogen. However, their similarity to the tight-binding functions discussed above leads to the expectation that the Wannier functions also appear as localized. This raises the question of whether they may be constructed in a maximally localized form.[31] It must be noted, however, that the formal construction of a Wannier function very much depends on the static approximation, something that might well be challenged for hydrogen.

To summarize: it is perfectly possible (and straightforward in a LCAO framework) to re-express the wave-functions of the crystal, i.e., those of the bands, in terms of linear combinations of bond orbitals (σ_g and σ_u*). And this is what we will do in the sequel, couching our discussion for dense hydrogen in terms of the population of these σ_g and σ_u* MOs of a single molecular fragment in the crystal. We do so fully aware that one must exercise care in attributing reality of these "local" populations; here the kind of observable being discussed is of considerable importance.

IV. THE CORRELATION BETWEEN INTRAMOLECULAR H-H SEPARATION, AND THE σ_g AND σ_u* H_2 FRAGMENT MO POPULATION

A. Depopulation of σ_g, and population of σ_u*

In the extended Hückel method,[20] the simplest of LCAO-MO implementations,[32] the electronic structure of a periodic solid is computed with a basis set of atomic functions rather than plane waves. Each crystal orbital is then expressed as a linear combination of those atomic functions. If one decomposes the macroscopic crystal into molecular fragments, each crystal orbital can be expressed, with no loss of detail, as a linear combination of the molecular orbitals of each fragment. These, in turn, are linear combinations of the atomic functions.

Pairs of hydrogens are the obvious fragments for a crystal of hydrogen below 490 GPa. Each H_2 carries two essential fragment molecular orbitals (neglecting higher principal quantum number combinations and continuum states): σ_g and σ_u*. These molecular orbitals develop into Bloch functions,

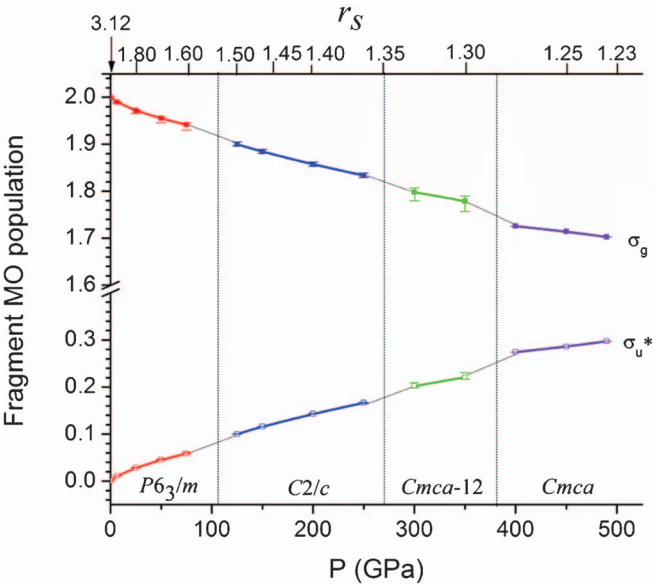

FIG. 4. Population of the fragment σ_g and σ_u* MOs in hydrogen as a function of pressure (averaged over the unit cell), as calculated by the extended Hückel method. Recall that at 490 GPa the relative compression is 15.8. The slight "spread bars" show the range of populations found.

in the usual way, thus becoming delocalized over the crystal. That is the starting point for a calculation, which then turns on the overlap between the crystal orbitals. The result of this interaction is that each basis Bloch function, σ_g or σ_u*, mixes into itself a little or a lot of the MOs (i.e., σ_g and σ_u*) of the other H_2s in the crystal. By summing the fractional occupancies of all the crystal orbitals and averaging over the first Brillouin zone, one can then obtain the total population of each fragment molecular orbital.

Using the Mulliken population analysis scheme,[33] we have computed the population of the fragments σ_g and σ_u* of the H_2 units involved in the different molecular structures of solid hydrogen at pressures ranging from 1 atm to 490 GPa, (or $3.12 < r_s < 1.23$). Since the molecular structures can involve non-equivalent H_2 pairs, we averaged these populations over the unit cell. The result is plotted in Figure 4. The Mulliken population analysis scheme is most probably the simplest of a number of atom partitions of the total density. And still one of the most popular despite its well-known weaknesses. In particular, it is basis-set dependent, and on occasion can give populations <0 and >2 in an orbital. Nonetheless, the Mulliken population analysis has been found to give good results for small basis sets such as the one used in the extended Hückel method. Its great advantage is its simplicity and transparency.

The average population of the σ_u* fragment MOs increases regularly with pressure, from 0.00 at 1 atm to 0.30 electrons at 490 GPa, while correspondingly the average population of the σ_g fragment MOs is depleted from 2.00. Thus, whereas an isolated H_2 molecule can be described (in a single configuration approximation) as $(\sigma_g)^{2.00}$ and $(\sigma_u^*)^{0.00}$, at 490 GPa the average over the whole crystal in hydrogen is $(\sigma_g)^{1.70}$ and $(\sigma_u^*)^{0.30}$. And no, there are no excited H_2 molecules in solid H_2 under pressure. But one way to think

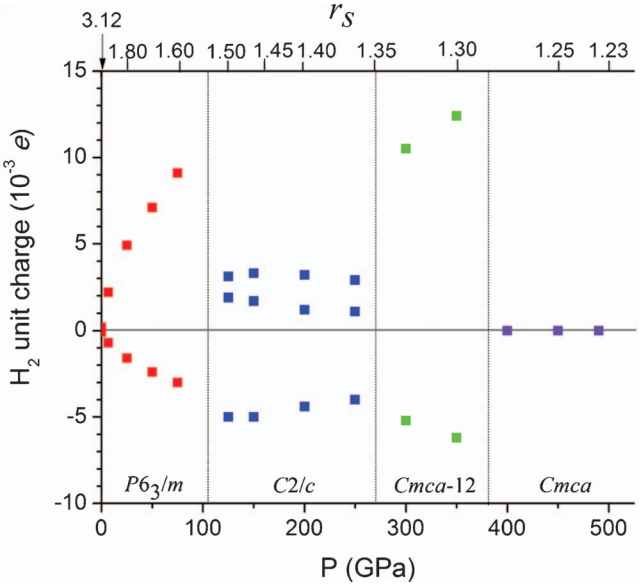

FIG. 5. Net charge of hydrogen pairs under pressure, as calculated using the extended Hückel method. Note the scale, in thousandths of an elementary charge e. Because the $P6_3/m$, $C2/c$, and $Cmca$-12 structures involve non-equivalent H_2 pairs in their unit cells, each type of H_2 is likely to be partially charged by a different amount. For example, at $P = 200$ GPa in the $C2/c$ structure, one third of the H_2 units bears 1.2×10^{-3} e, a second third bears 3.2×10^{-3} e, and the last third bears -4.4×10^{-3} e.

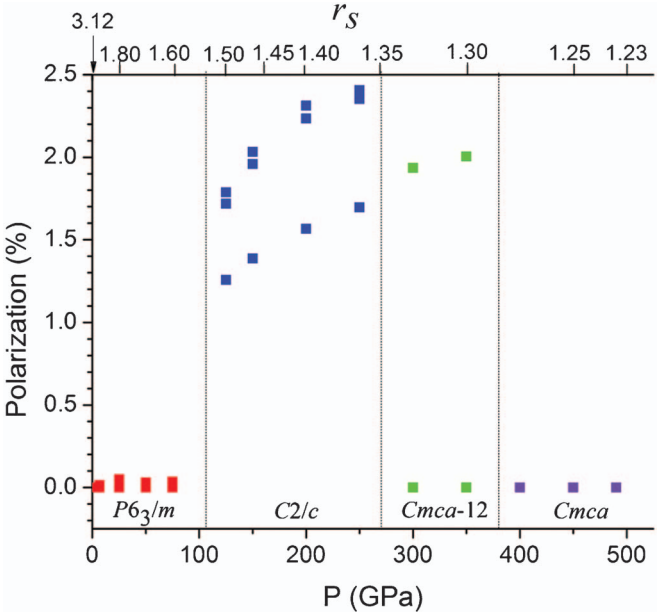

FIG. 6. Evolution of the H_2 molecules polarization under pressure. The polarization of each H_2 molecule is estimated by using (see text) the formula $Polarization\,(\%) = \frac{|(1-q(H_A))-(1-q(H_B))|}{2-q(H_A-H_B)} \times 100$, where, respectively, $q(H_A)$, $q(H_B)$, and $q(H_A - H_B)$ are the partial charges held by the H atoms H_A and H_B, and by the H_2 molecule H_A-H_B.

about this is that the interaction of a given H_2 with its neighbors has led to an effective partial excitation of the H_2.

The perspective above has been a productive one for molecules, from the early days of organometallic chemistry. By way of example and comparison, an ethylene complex $L_nM(C_2H_4)$ could be seen as containing an effectively partially excited ethylene, some fraction of an electron in it promoted from the π to π^* orbital. The bond lengths and force constants of the coordinated ethylene could then be related to the properties of an excited ethylene.

B. Intermolecular charge transfer

Going further, and mainly because the structures considered contain non-equivalent H_2 units, there is a small amount of charge transfer from some pairs to others. Figure 5 presents the net charges of the H_2 pairs in the four molecular structures cited earlier. The vertical scale is in 10^{-3} of an elementary charge e.

It is in the $P6_3/m$ and $Cmca$-12 structures, where hydrogen pairs with quite different environments are found (see Figure 1), that one finds the greatest degree of charge transfer. In absolute terms, the charge transfer from some molecules to others is very small. And it is in the $Cmca$-12 structure at 350 GPa that individual H_2 units with the largest charges in absolute value are found, and even that is small ($+0.013e$). Given this relative lack of "charging" of individual H_2 units in any phase, it is more appropriate to formally describe hydrogen under pressure as an ensemble of partially "excited" H_2 molecules, rather than as a mixture of partially charged H_2^+ and H_2^- ions.

C. Polarized H_2 molecules in some structures, in particular candidate structures for Phase III

Of course, the lack of total electron transfer does not imply that the H_2 units are un-polarized. This can be seen in Figure 6, which shows the evolution of the average polarization of the H_2 units under pressure in the $P6_3/m$, $C2/c$, $Cmca$-12, and $Cmca$ structures. In this plot, the polarization is defined as

$$Polarization\,(\%) = \frac{|(1 - q\,(H_A)) - (1 - q\,(H_B))|}{2 - q\,(H_A - H_B)} \times 100,$$

where, respectively, $q(H_A)$, $q(H_B)$, and $q(H_A - H_B)$ are the partial charges computed for the H atoms H_A and H_B, and for the H_2 molecule H_A-H_B, according to a Mulliken population analysis in the extended Hückel model.

In the $P6_3/m$ and $Cmca$ structures, the H_2 molecules are un-polarized, a consequence of the fact that in these structures both protons of each hydrogen pair have the same environment (see Figure 1). By contrast, in the $C2/c$ and $Cmca$-12 structures, the hydrogens in the pairs are not equivalent (see Figure 1), resulting in a net polarization of the pairs. For example, at P = 150 GPa ($r_s = 1.46$) in the $C2/c$ structure, one third of the H_2 units are polarized by 1.4%, a second third by 1.9%, and the last third by 2.0%. Note that at about the same compression, ($r_s = 1.47$), Edwards and Ashcroft computed a spontaneous polarization of the H_2 units of the same order – about 1% – for the orthorhombic $Cmc2_1$ structure.[34]

This polarization appears stronger in the $C2/c$ structure than in $Cmca$-12. It is worth noting that the $C2/c$ structure is proposed by Pickard and Needs as a good candidate for the H-A phase (or Phase III) of hydrogen, experimentally characterized by strong IR activity, rising steadily with pressure. Theoretical studies of the spectroscopic properties of this polarized

structure have already been reported.[9,34,35] Figure 5 shows that the H_2 molecules in the $C2/c$ structure have a polarization of 2% at 200 GPa. This corresponds to an average static charge of $0.021e$ for the hydrogen atoms of the H_2 molecules, almost neutral by themselves. This is in reasonable agreement with the Szigetti effective charge of $0.038e$ deduced experimentally from the IR vibron of Phase III of hydrogen at the same pressure.[36] Evidently one does not need very much polarization to make the appearance of the IR H_2 vibron quite prominent.

D. A linear relationship

We know from our previous studies[2] that the intramolecular H-H separation in crystalline hydrogen is remarkably unaffected by increase of density (remaining low, and close to 0.75 Å), given the large calculated population transferred from σ_g to σ_u* fragment MOs of the H_2 units. Let us see if we can make this more precise. We can define a measure of the "ideal" intramolecular H-H separation associated with given σ_g and σ_u* populations, neglecting all effects other than orbital interactions and (neglecting, but temporarily, the effect of spatial confinement), just by assuming a linear relation between the intramolecular H-H separation of a "partially excited" H_2 molecule and the population δ transferred from its σ_g to its σ_u*, given by the following equation:

$$l(H_2^{\delta\ddagger}) = l(H_2) + \delta\{l(H_2^{\ddagger}) - l(H_2)\}. \quad (1)$$

Here $l(H_2^{\delta\ddagger})$ is the intramolecular H-H separation of a H_2 molecule having its σ_g and σ_u* MOs occupied by $(2-\delta)$ and δ electrons, respectively, and $l(H_2^{\ddagger})$ and $l(H_2)$ are the intramolecular H-H separations of a H_2 molecule in its $^1\Sigma_u^+$excited state ($l(H_2^{\ddagger})$ = 1.29 Å) and $^1\Sigma_g$ ground state ($l(H_2)$ = 0.74 Å), respectively, as in a dilute gas phase at 1 atm.

Put in basic terms, Eq. (1) expresses the tuning of the paired hydrogen separation as the outcome of two factors. First, one imagines a hydrogen molecule undergoing a charge transfer from its σ_g to its σ_u* state, to give the "partially excited" molecule. Then one models the interatomic separation in a partially excited H_2 molecule as a "linear combination" between its ground and excited forms. The validity of this approximation has been checked for the model shown in Figure 7 where two H_2 molecules are linearly aligned. In this system, by fixing the intermolecular H-H separation d, we can control the overlap, and thus interaction, between the σ_g MO of one H_2 molecule and the σ_u* MO of the second molecule (and vice versa). The net result will be that by varying d we

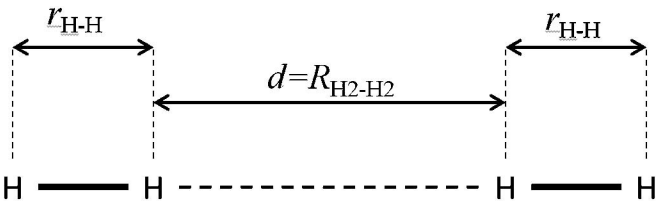

FIG. 7. Two H_2 molecules along a line, the molecular model considered in studying the relation between H_2 bond length and σ_u* population.

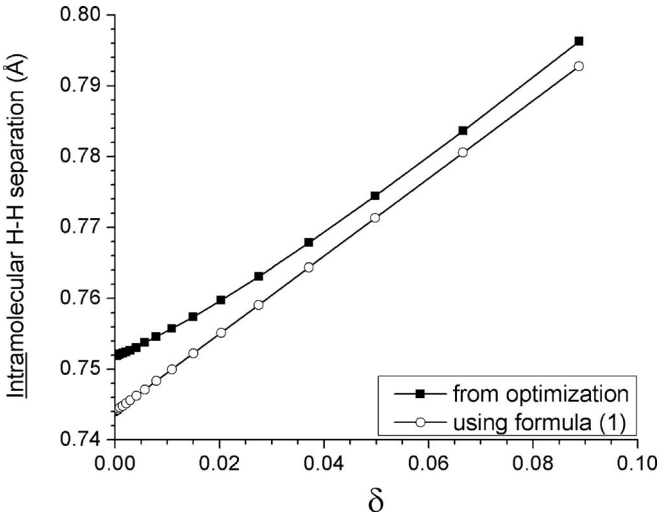

FIG. 8. Intramolecular H-H separation, optimized by DFT (filled squares) and also given by formula (1) (empty circles) plotted as a function of δ, this being the population transferred from σ_g to σ_u* for the system given in Figure 7.

can control the fraction of an electron transferred from the σ_g to the σ_u* MOs. Note that the overall size (here the length) of the system is not constrained. We believe this is a suitable model to establish the relationship between intramolecular H-H separation and MO population, decoupled from any other effect, and from the applied external pressure, in particular.

The intramolecular H-H separation $r_{H\text{-}H}$ has been optimized for different values of the intermolecular separation d by DFT at the PBEPBE/6-311++G(d,p) level of theory. In Figure 8 is plotted the ensuing optimal intramolecular H-H separation $r_{H\text{-}H}$ and that given by formula (1); the σ_g and σ_u* populations are evaluated once again by the extended Hückel method.[20]

The relation between the intramolecular H-H separation and the population transferred from σ_g to σ_u* first of all appears linear, over quite a wide range of δ. Furthermore, formula (1) also provides a good model for the intramolecular H-H distance. Indeed, in the range plotted in Figure 8, the agreement is better than 1%. Part of the difference between the optimized bond length and that given by formula (1) can be readily attributed to the tendency of the PBE functional to overestimate bond lengths.[37]

V. GIVEN THE ORBITAL POPULATIONS, THE INTRA-MOLECULAR H-H SEPARATIONS IN COMPRESSED HYDROGEN ARE SHORTER THAN THEY SHOULD BE

Armed with a formula that now relates intramolecular H-H separation to orbital occupation, we can return to the computed Pickard and Needs H_2 structures. The application of formula (1) in the case of $P6_3/m$, $C2/c$, $Cmca$-12, and $Cmca$ structures is plotted in Figure 9. The actual intramolecular H-H separation in solid hydrogen is much shorter (by ~14% at 490 GPa) than expected from the σ_g fragment MO depopulation and σ_u* fragment MO population of the H_2 molecules. At 490 GPa ($r_s \sim 1.23$) the intramolecular H-H separation calculated using formula (1) is still shorter than the average

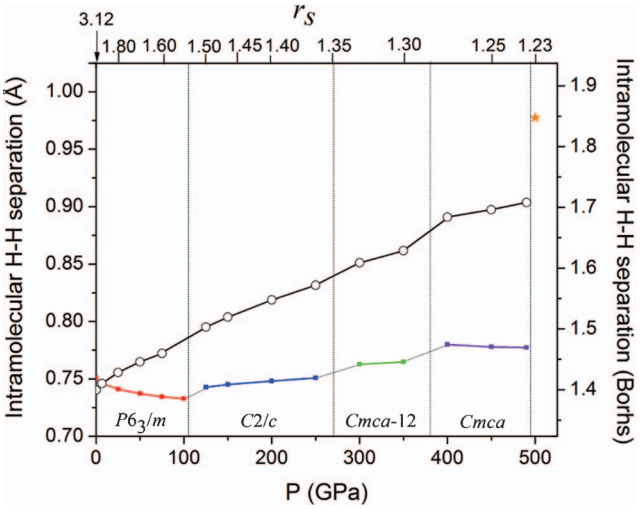

FIG. 9. Average computed intramolecular H-H separation in hydrogen under pressure (filled squares) and average intramolecular H-H separation as calculated according to Eq. (1) (empty circles).

shortest intermolecular H-H separation, which is 1.0 Å. Nevertheless, from a purely orbital point of view, the degree of equalization of the intra- and intermolecular H-H separations is achieved to a greater degree than one would have anticipated.

What, therefore, is the reason for the notable discrepancy apparent in Figure 9, namely, the intramolecular H-H distances in various H_2 phases are progressively shorter (as the pressure increases) than they "should be" from the depopulation of their σ_g levels and population of their σ_u* counterparts? We propose that what pushes the upper curve in Figure 9 down into the lower one is the physical/confinement effect proposed in the second paper of this series.[10] The intramolecular H-H separations "want to be" longer (from σ_u* population, and σ_g depopulation); but the pressure, via encroaching neighbors, tends to make them shorter.

One supporting piece of evidence (if indirectly so) for the idea that the intramolecular H-H separations are shorter than they "should be" is that in the organometallic di-hydrogen complexes mentioned in the second paper of this series,[10] the H-H distances are typically 0.82–0.89 Å and even longer. In these $P = 1$ atm complexes there is no pressure active on a chemically elongated H_2. And the H_2 units indeed stretch.

This idea can also be illustrated with a very simple molecular model: going back to our two H_2 molecules sketched in Figure 7, we now place two helium atoms at each extremity of the collinear arrangement, which leads to the system sketched in Figure 10.

The He atoms act as a "soft" wall surrounding the pair of H_2 molecules. In this system, each H_2 molecule is confined between one He atom and the other H_2 molecule, and, in addition, the two H_2 molecules interact with each other. In this system, as in solid hydrogen, the physical and chemical effects affecting the intramolecular H-H separation are both operative. For several fixed distances $d_{wall\text{-}wall}$ between the He atoms, the intermolecular ($R_{H_2\text{-}H_2}$) and intramolecular ($r_{H\text{-}H}$) H-H separations in this small system have been simultaneously optimized by DFT at the PBEPBE/6-311++G(d,p)

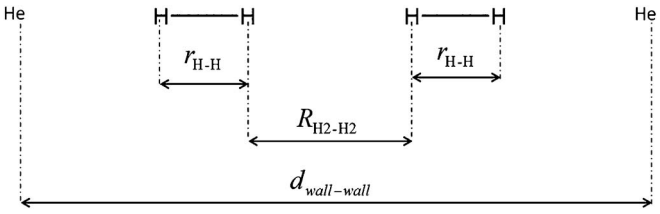

FIG. 10. Two H_2 molecules along a line, surrounded by two helium atoms, the molecular model considered to illustrate the concomitant effect of spatial confinement and orbital interaction.

level of theory. As expected, as $d_{wall\text{-}wall}$ decreases (a surrogate for pressure increasing), the intermolecular H-H separation $R_{H_2\text{-}H_2}$ decreases. The concomitant evolution of the intramolecular H-H separation $r_{H\text{-}H}$ is plotted in Figure 11 with respect to the intermolecular H-H separation $R_{H_2\text{-}H_2}$ (black squares). The intramolecular H-H separation shortens as the intermolecular H-H separation decreases – an indication of the fact that the spatial confinement effect is rather strong in this arrangement.

We now remove the He atoms. The H_2 molecules are no longer confined (except on the "inside," between the two molecules), yet they still interact with each other, through orbital overlap. The intramolecular H-H separations have been re-optimized with the same methodology for several fixed intermolecular H-H separations; the evolution of $r_{H\text{-}H}$ with $R_{H_2\text{-}H_2}$ is shown in Figure 11 (red circles). The suppression of spatial confinement (on the outside) leads to a lengthening of the intramolecular H-H separation – an effect that increases as the intermolecular H-H separation decreases. This elongation is due solely to orbital interactions, i.e., to the overlap between orbitals of both molecules. Thus, the gap between black squares and red circles in Figure 11 at a given intermolecular H-H separation ($R_{H_2\text{-}H_2}$) is a measure of the strength of

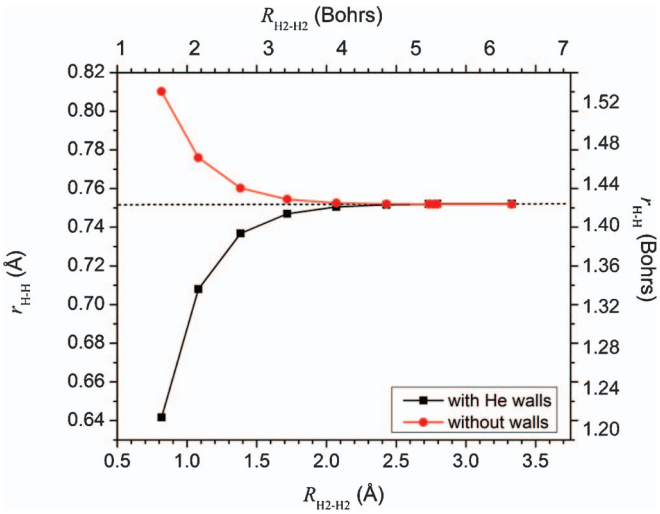

FIG. 11. Effect of the presence of two He atoms surrounding a collinear arrangement of two interacting H_2 molecules (see Figure 10) on the intramolecular H-H separation. Black squares represent the evolution of the optimal intramolecular H-H separation with the intermolecular H-H separation when He atoms are present and red circles the same quantity when He atoms have been removed.

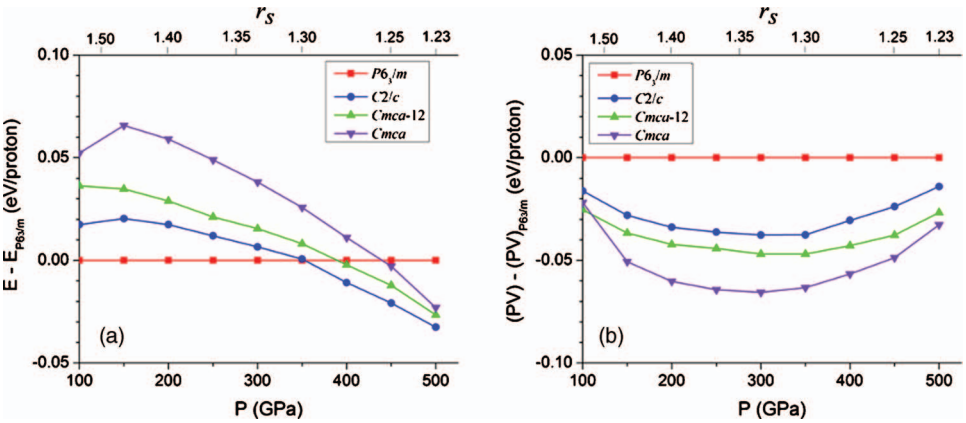

FIG. 12. E, (a) and PV, (b) contributions to the enthalpy H per proton of the $P6_3/m$, $C2/c$, $Cmca$-12, and $Cmca$ structures between 100 GPa and 500 GPa, (r_s = 1.54 and 1.23) here plotted with respect to their values in the $P6_3/m$ structure.

the physical/confinement effect operating "on top of" orbital interactions.

VI. SO WHY DO STRUCTURES BECOME PREFERRED?

Under pressure, the structure of hydrogen clearly evolves. To better understand why one structure is eventually favored over another at a pressure P we are now going to look at the intrinsic differences between the $P6_3/m$, $C2/c$, $Cmca$-12, and $Cmca$ structures but at a given pressure and again in a static approximation.

A. *E* and *PV* contributions to the enthalpy *H*

First let us separate the internal energy E and PV contributions to the enthalpy H. Our focus is on the pressure regime where the intramolecular H-H separation starts to increase with pressure, from 100 GPa to 500 GPa, a range of pressure in which MO overlap becomes substantial. In Figures 12(a) and 12(b) are plotted the E and PV energy contributions to the enthalpy of the $P6_3/m$, $C2/c$, $Cmca$-12, and $Cmca$ structures in this pressure regime. Recall that as the pressure increases, the calculated enthalpy of the structures evolves according to the order given in Table I, namely, $P6_3/m \rightarrow C2/c \rightarrow Cmca-12\rightarrow Cmca$.

For a given structure, it is expected that as pressure increases, the internal energy E should increase. It also appears from Figures 12(a) and 12(b) that at a given pressure, the structures which are the most favored by their PV contributions are disfavored by their internal energy E. As expected, the $P6_3/m$ structure, which is the most stable at lower pressures, is globally "E-favored" but "(PV)-disfavored" relative to the others. In some contrast, the $Cmca$ structure, which is the most stable at higher pressures, is E-disfavored energetically but (PV)-favored. The $C2/c$ and $Cmca$-12 structures exhibit intermediate behavior.

B. A microscopic view

Now let us try to establish the effects of energy and volume in terms of the detailed separations in the structures. Figure 13(a) shows the intermolecular separations for the four structures over the entire pressure range, and Figure 13(b) the corresponding intramolecular distances. In the supplemental material to this paper, Figure S1,[38] we also show the fractional number of electrons transferred from the σ_g fragment MO of the H_2 molecules to σ_u*; this, in general, goes along with the intramolecular separation variation.

Note first of all that the intermolecular separations (Fig. 13(a)) correlate in a general way with the PV terms (Fig. 10(b)) – the $P6_3/m$ structure has the longest separations,

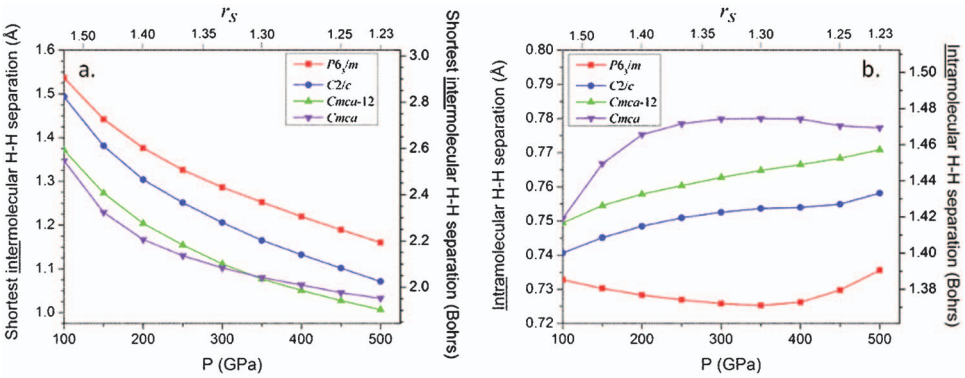

FIG. 13. (a) Average shortest intermolecular H-H separation; (b) Average intramolecular H-H separation of the H_2 units in the $P6_3/m$, $C2/c$, $Cmca$-12, and $Cmca$ structures between 100 GPa and 500 GPa (r_s = 1.54 and 1.23). Note the separation scales are very different for the two graphs.

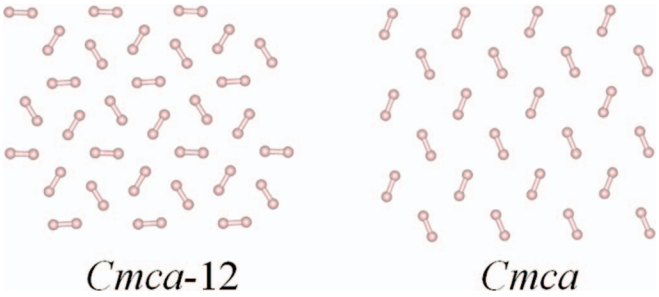

FIG. 14. Relative orientation of H_2 units in the *Cmca*-12 and *Cmca* structure (here in the *ab* and *bc* planes, respectively).

the *Cmca*-12 and *Cmca* structures have the shortest. Density is not directly related to just a single intermolecular separation in a three-dimensional array – in a general way packing also matters. Figure 14 shows the relative orientation of the molecules in the two structures competing at the highest density, *Cmca*-12 and *Cmca.* Packing efficiency is not obvious; the *Cmca* structure attains a higher density, while (Fig. 13(a)) the shortest intermolecular separation does not distinguish it from its *Cmca*-12 competitor.

The intramolecular separations (Figure 13(b)) introduce a surprise – the longest bonds (with associated electron transfer from σ_g to σ_u*) are those associated with the two structures that achieve the highest density, and so are the more stable at higher pressures; these are *Cmca*-12 and *Cmca*. Here, as in the case of other molecules such as ice-X, molecules go through complex re-arrangements as they are induced to higher densities – they move closer together, which (through orbital interactions) weakens some bonds in the structure. These bonds stretch, even when others contract. The overall density must necessarily increase with increasing pressure, but individual nuclear separations need not necessarily contract uniformly.

VII. CONCLUSION

A fragment molecular orbital analysis of those structures predicted by Pickard and Needs to be most stable for the ground state of static solid hydrogen at high pressures, coupled with a molecular model, provides a detailed chemical/physical account of the complex interactions that take place in this deceptively simple system. Our analysis indicates that as pressure increases, the σ_g fragment MOs of the H_2 units depopulate and correspondingly the σ_u* fragments are populated. The H_2 units become polarized in some of the phases, but the net charge transfer between two H_2 units still appears to be very small up to 300 GPa. A molecular model of this character gives us a way to quantify the expected bond length elongation for a given amount of electron transfer from the $\sigma_g \rightarrow \sigma_u$* orbitals.

Applying this model to the solid hydrogen phases indicates that the intramolecular H-H separations are much shorter than they are expected to be, in fact, increasingly so at higher pressure. We argue that two effects coexist and compete: spatial confinement of the molecules which tends to shorten and stiffen the intramolecular H-H bond, and the orbital interactions between neighboring H_2 units, which tend to transfer electrons from the σ_g MO of the molecules to their σ_u* counterparts, lengthening and weakening the intramolecular bond. We are also able to tease apart the relative energy and *PV* contributions to the differential stabilization under pressure of the various phases.

In this paper, as in the first two of this series, we have mined the Pickard and Needs numerical data set and, focusing in particular on the H-H separations, we extracted from the static calculations as much as we could about the chemical and physical factors driving the changes in the structure of hydrogen under pressure. In the fourth and last paper in the series[39] we will conclude by seeking something quite different, still in the spirit of building models to gain understanding, but now looking at the equalization problem from a different perspective. Rather than examining the best candidate structures for hydrogen under pressure, we will construct a simple pathway from the molecular low-coordination extreme to the high pressure high-coordination monatomic regime, and even higher than the 500 GPa structures we have discussed so far. This itinerary for bond equalization and increase in coordination will pass through geometries that may not be at each point as low in enthalpy as the optimized structures. But the pathway to be introduced will have an advantage of simplicity, while capturing the essence of increase in coordination that must accompany any increase in density. We also expect (and will) gain useful information from the associated enthalpy changes.

[1]E. Wigner and H. B. Huntington, J. Chem. Phys. **3**, 764 (1935).
[2]V. Labet, P. Gonzalez-Morelos, R. Hoffmann, and N. W. Ashcroft, J. Chem. Phys. **136**, 074501 (2012).
[3]P. Loubeyre, M. Jean-Louis, and I. F. Silvera, Phys. Rev. B **43**, 10191 (1991).
[4]I. F. Silvera and R. J. Wijngaarden, Phys. Rev. Lett. **47**, 39 (1981).
[5]F. Grazzi, M. Moraldi, and L. Ulivi, Europhys. Lett. **68**, 664 (2004).
[6]S. K. Sharma, H. K. Mao, and P. M. Bell, Phys. Rev. Lett. **44**, 886 (1980).
[7]S. K. Sharma, H. K. Mao, and P. M. Bell, Phys. Rev. Lett. **46**, 1109 (1981).
[8]R. J. Hemley and H. K. Mao, Phys. Rev. Lett. **61**, 857 (1988).
[9]C. J. Pickard and R. J. Needs, Nat. Phys. **3**, 473 (2007).
[10]V. Labet, R. Hoffmann, and N. W. Ashcroft, J. Chem. Phys. **136**, 074502 (2012).
[11]G. Kresse and J. Hafner, Phys. Rev. B **47**, 558 (1993).
[12]G. Kresse and J. Furthmüller, Comput. Mater. Sci. **6**, 15 (1996).
[13]G. Kresse and J. Furthmüller, Phys. Rev. B **54**, 11169 (1996).
[14]J. P. Perdew, K. Burke, and M. Ernzerhof, Phys. Rev. Lett. **77**, 3865 (1996).
[15]J. P. Perdew, K. Burke, and M. Ernzerhof, Phys. Rev. Lett. **78**, 1396 (1997).
[16]P. E. Bloch, Phys. Rev. B **50**, 17953 (1994).
[17]G. Kresse and D. Joubert, Phys. Rev. B **59**, 1758 (1999).
[18]J. M. MacMahon and D. M. Ceperley, Phys. Rev. Lett. **106**, 165302 (2011).
[19]H. J. Monkhorst and J. D. Pack, Phys. Rev. B **13**, 5188 (1976).
[20]R. Hoffmann, J. Chem. Phys. **39**, 1397 (1963).
[21]G. A. Landrum, W. V. Glassey, BIND (version 3.0). BIND is distributed as part of the YAeHMOP extended Hückel molecular orbital package and is freely available on the WWW at http://sourceforge.net/projects/yaehmop/.
[22]M. J. Frisch, G. W. Trucks, H. B. Schlegel *et al.*, GAUSSIAN 03, Revision B.04, Gaussian, Inc., Pittsburgh, PA, 2003.
[23]C. Edmiston and K. Ruedenberg, Rev. Mod. Phys. **35**, 4571 (1963).
[24]S. F. Boys, Rev. Mod. Phys. **32**, 296 (1960).
[25]J. M. Foster and S. F. Boys, Rev. Mod. Phys. **32**, 300 (1960).
[26]J. Pipek and P. Mezey, J. Chem. Phys. **90**, 4916 (1989).
[27]W. L. Luken and D. N. Beratan, Theor. Chim. Acta **61**, 265 (1982).
[28]G. Wannier, Phys. Rev. **52**, 191 (1937).
[29]M. R. Geller and W. Kohn, Phys. Rev. B **48**, 14085 (1993).

[30]N. W. Ashcroft and N. D. Mermin, in *Solid State Physics* (Saunders, Philadelphia, 1976).
[31]For some recent developments, see J. R. Yates, X. Wang, D. Vanderbilt, and I. Souza, Phys. Rev. B **75**, 195121 (2007).
[32]For a succinct description of the method, and its relationship to perturbed free-electron models, see R. F. Berger, P. L. Walters, S. Lee, and R. Hoffmann, Chem. Rev. **111**, 4522 (2011).
[33]R. S. Mulliken, J. Chem. Phys. **23**, 1833 (1955).
[34]B. Edwards and N. W. Ashcroft, Nature (London) **388**, 652 (1997).
[35]J. S. Tse, D. D. Klug, Y. Yao, Y. Le Page, and J. R. Rodgers, Solid State Commun. **145**, 5 (2008).
[36]R. J. Hemley, I. I. Mazin, A. F. Goncharov, and H.-k. Mao, Europhys. Lett. **37**, 403 (1997).
[37]G. Menconi and D. J. Tozer, Chem. Phys. Lett. **360**, 38 (2002).
[38]See supplementary material at http://dx.doi.org/10.1063/1.3679749 for this figure.
[39]V. Labet, R. Hoffmann, and N. W. Ashcroft, J. Chem. Phys. **136**, 074504 (2012).